JJEE

Volume X | Number X | Month 20XX | Pages XXX-XXX

Jordan Journal of Electrical Engineering

ISSN (print): 2409-9600, ISSN (online): 2409-9619

Homepage: jjee.ttu.edu.jo

Location of Faults in Six Phase Transmission Line using a Neuro Fuzzy System

A. Naresh Kumar[1*], M. Ramesha[2], Elemasetty Uday Kiran[3], M. Suresh Kumar[4], Malleboina Nagaraju[5], M. Chakravarthy[6], Bharathi Gururaj[7]

[1] Department of Electrical and Electronics Engineering, Institute of Aeronautical Engineering, Hyderabad, India
E-mail: ankamnaresh29@gmail.com
[2] Department of Electrical, Electronics and Communication Engineering, Gandhi Institute of Technology and Management, Bengaluru, India
[3] Department of Aerospace Engineering, Toronto Metropolitan University, Toronto, Canada
[4] Department of Space Engineering, Ajeenkya DY Patil University, Pune, India
[5] Department of Information Technology, University of the Cumberlands, Williamsburg, USA
[6] Department of Electrical and Electronics Engineering, Vasavi College of Engineering, Hyderabad, India
[7] Department of Electronics and Communication Engineering, ACS College of Engineering, Bengaluru, India

Received: Sep 16, 2023 *Revised: Oct 22, 2023* *Accepted: Oct 27, 2023* *Available online: Jun 2, 2024*

***Abstract*—** Fault location plays an important role in power systems. It is frequently used in transmission lines to reduce the system damage for growing electrical energy demand. However, the location estimation method itself is easy to be disturbed by different parameters and gives estimation errors. To solve this problem, this paper introduces a scheme that uses neuro fuzzy system (NFS) to locate all types of faults such as shunt faults, transforming faults, series faults and simultaneous faults in six phase overhead line (SPOL). This scheme has been performed on a 68 km, 138 kV, 60Hz, SPOL for all fault types by employing MATLAB software Simulink. Here, Haar wavelet transforms (HWT) are used to extract the current signals in order to evaluate the behavior and characteristics of higher frequency components. Then, the obtained HWT currents data are employed to construct the fault location scheme in SPOL based on NFS. The obtained experimental results confirm that by using the NFS, the maximum fault location error (MFLE) can be reduced by more than 10%. It can further reduce the maximum response time (MRT) for the operator to address the faults and ensure the power system reliability in the future. The test result executed in this investigation indicates that the NFS is resilient to wide changes in fault conditions, and it shows good performance and huge potential for location of faults in SPOL.

***Keywords*—** Fault location; Neuro fuzzy system; Six phase transmission line; Haar wavelet transform.

1. RESEARCH GAP AND MOTIVATION

With the continuous development of India's economy, the cultural level and material living standards of the society is increasing, and the necessities for the safety of the electrical power system are getting higher and higher. The transmission line disconnection will have a huge effect on society lives. Owing to the wide transmission line coverage, natural conditions and human factors have caused many issues in power system operation and maintenance. With the large future achievements in transmission lines and limited access to right of ways, higher power density transmission models will be essential. One of which is higher phase order technology i.e. six phase overhead line (SPOL), which has been shown to transfer more amount of power for less right of way. Another transmission line, i.e., high voltage direct current line, needs huge amount capital investment for installation process and its maintenance of power system. In this context, SPOL has been planned to meet growing electrical demand. A series of

* Corresponding author
DOI: https://doi.org/10.5455/jjee.204-1694875095

reports has been published to design SPOL structure [1-3]. There is no fault-free transmission line and it is neither economical nor practical to made a fault-free transmission line. So far, there are several methods for location of shunt faults in SPOL [4, 5]. Shunt fault location in SPOL has been widely studied using single end data [6, 7]. Until now, numerous approaches, offered to estimate the fault protection on SPOL [8-16]. However, recent research studies found that there are still some issues in SPOL.

Up to now, number of tools like artificial neural networks (ANN) [17], k-nearest neighbor algorithm [18], dual vector control technique [19] and random forest regressor [20] have been used for locating shunt faults. The algorithm is the improvement of the shunt fault location method presented using haar wavelet transforms (HWT) currents [21]. A wide application of support vector machine (SVM) for shunt fault location of transmission line from single end data has been seen in recent literature [22]. ANN based model with better performance of shunt faults on SPOL have been introduced in [23]. Some of the researchers have analysed a solution to the problems of transforming faults [24, 25]. Application of time-domain algorithm for transforming fault location has been developed in [26]. A method for transforming fault location which uses sparse wide area measurements was proposed in [27]. As an application, transforming fault location in transmission lines using single end current data was subject of few research [28, 29]. Soft computing method plays a main role for series fault location applications. There have been some reports studying the series faults of transmission line [30, 31]. Several researchers have presented the series faults without considering the voltages [32, 33]. Relevant experts have done a lot of research on how to detect under the condition of series faults [34]. Very few researchers have carried out series fault from current study for detection [35, 36]. A common research question in fault research is to locate simultaneous faults in transmission line [37-39]. Although fuzzy logic (FL) has been applied for simultaneous fault location in several works [40, 41]. Only a few publications have concerned simultaneous faults from single end current data [42, 43]. Till date of writing this manuscript, FL model has developed which uses HWT coefficients in [44].

One technique, which is employed nowadays widely, is neuro fuzzy system (NFS) which requires a minimal assumption. Currently, NFS is mostly focused on the location of transmission lines in the existing studies [45-47]. To achieve acceptable maximum fault location error (MFLE) in fault location for transmission line, applying the NFS has been recommended. There are many reference papers published for the location of faults in transmission lines from source end data using NFS [48-52]. However, a few references are focused for the location of faults using currents based on NFS. This can also be employed for the location of the line for shunt faults [53, 54], transforming faults [55] and simultaneous faults [56]. As per survey of existing reported methods for fault location of SPOL, it is found that, none of the previous approaches provide shunt faults, transforming faults, series faults and simultaneous faults considering HWT currents and NFS. In this scenario, the fault location model must be designed to identify the location for all types of faults in SPOL. This problem is tricky because transforming, series and simultaneous faults occurring in multiple phases may yield different results. The purpose of this paper is to design an efficient fault location scheme in SPOL considering NFS and HWT currents. Indeed, the core idea of this work is to minimize the MFLE. It does not use voltages and there is no need receiving terminal data. Moreover, this approach need only currents from source end that are presented in the current work. The remainder of this article is organized as follows. Related works about this article are reviewed in “Research

Gap and Motivation" Section. The SPOL simulation are presented in Section "Data Generation". Section "Neuro Fuzzy System" describes the design of NFS for fault location in SPOL. Section "Experimental Results" examines the performance of the NFS scheme. In the "Conclusion" Section, the results are summarized.

2. DATA GENERATION

The proposed NFS based location scheme has been implemented for a SPOL referring to the McCalmont-Springdale line length 68-km, 138 kV, 60 Hz as shown in Fig. 1. The sending end source impedance and receiving end source impedance are 2.13 + j9.14 Ω and 4.1 + j17.84 Ω, respectively. Two energy sources, 138kV, Source-1-and 138kV, Source-2 are present at bus-1 and bus-2, respectively. Two loads, 80 MW and 240 MW, are installed at bus-1 and bus-2, respectively. Corresponding to the HWT current waveforms for shunt faults, transforming faults, series faults and simultaneous faults in SPOL with time domain are simulated. Fig. 2, describes shunt fault that CDE fault at 52 km in 45 ms time. As illustrated in Fig. 2, fault current magnitude is same in (A, B and F lines) but fault magnitudes (C, D and E lines) are dissimilar i.e. increases. To study the effect of transforming faults on the six-phase current waveform that initially CD fault at 52 km in 45 ms time is transformed after 62 ms to CDE fault at the same location as shown in Fig. 3.

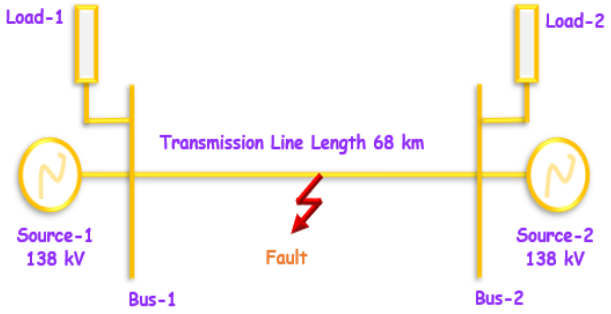

Fig. 1. SPOL Single line diagram implementation.

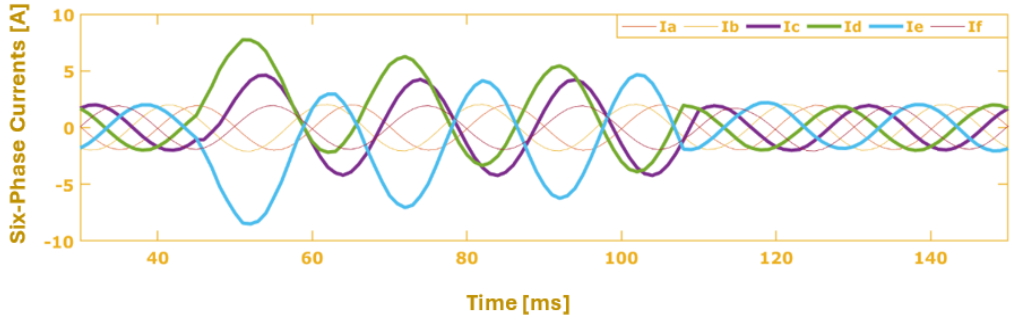

Fig. 2. Shunt fault currents in SPOL.

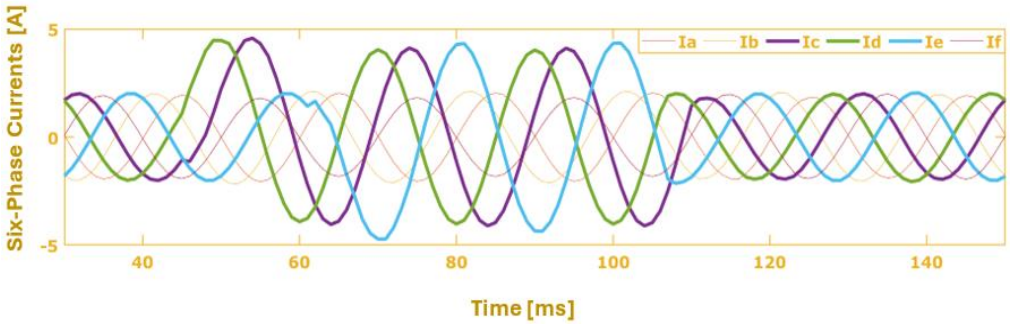

Fig. 3. Transforming fault currents in SPOL.

The current waveform during "bc" fault at 52 km in 105 ms time is depicted in Fig. 4. As exemplified in Fig. 4, fault current magnitude is same in ("A", "D", "E" and "F" lines) but fault magnitudes ("b" and "c" lines) are dissimilar i.e. decreases. Fig. 5 shows a simultaneous fault during "Ag-c" fault at 52 km in 45 ms time where the current waveform of phases is distorted by a sudden increase (in "A" line and ground) and decrease ("c" line) in their magnitude. Total 25 SPOL operating cases during healthy condition, variation in fault location (1, 5, 10, 20, 30, 40, 50, 60 and 67 km), variation in fault resistances (10, 20, 30, 40, 50 and 60), and variation in fault inception angles (0, 90 and 180) are considered. Thus, total samples simulated for the training data are 3035. These currents are used as inputs for NFS. The block diagram of the HWT-NFS SPOL faults is shown in Fig. 6. It is explained briefly in the flow diagram to better understand the implementation process of the NFS model in depicted Fig. 7. The possible faults in SPOL are explained in Fig. 8.

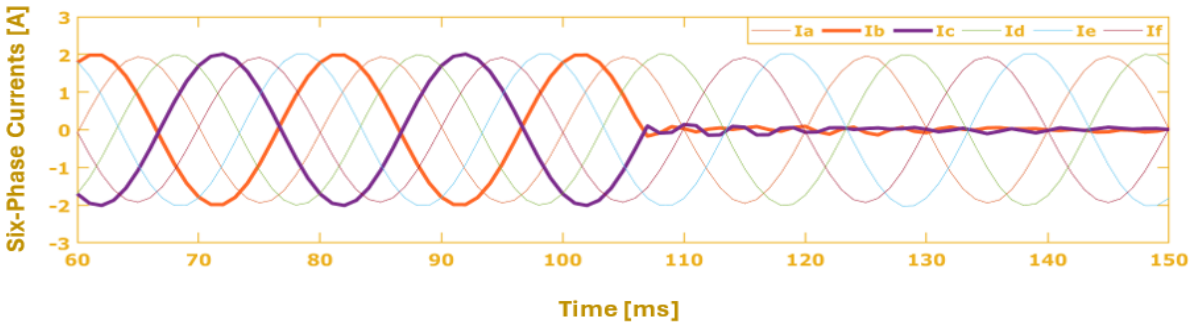

Fig. 4. Series fault currents in SPOL.

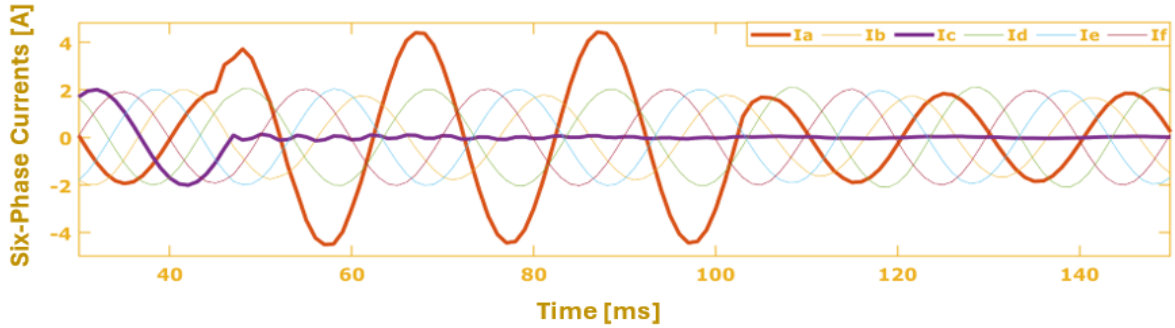

Fig. 5. Simultaneous fault currents in SPOL.

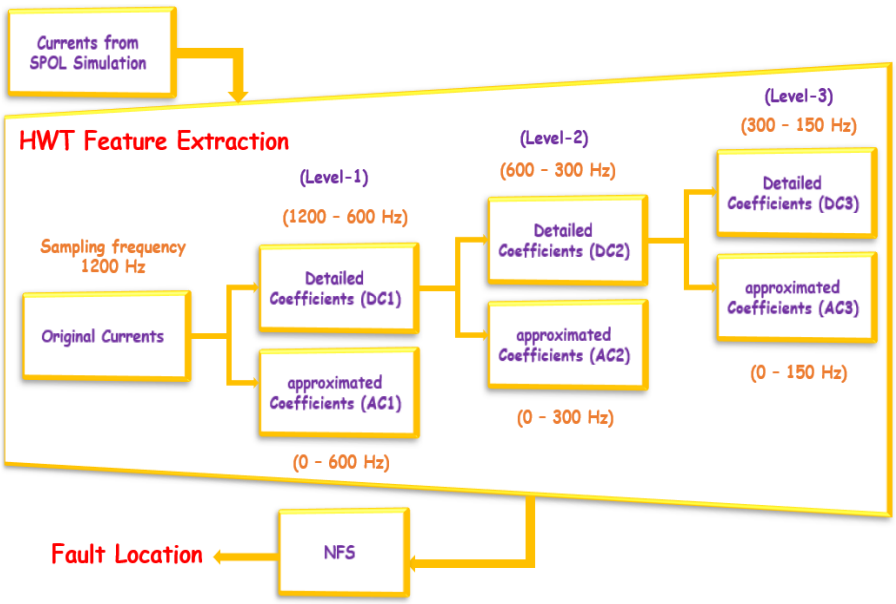

Fig. 6. Block diagram of the HWT-NFS SPOL faults.

Fourier transform only supports stationary signals whereas wavelet transform is an effective tool for evaluating transient nonstationary signals. One of the simplest wavelets transform family is the HWT and is the member of rectangular waveform orthogonal family whose peak value changes with function. It is also a mathematical transformation function employed in fault analysis, signal processing study, medical and image analysis. It is applied to these sampled data to derive the small-grained (detailed and approximated coefficients) detail of the signal. Here, 3rd level of HWT is applied for feature extraction (detailed and approximated coefficient) from the current signals of the SPOL. The NFS operation is based on the transient current's multiresolution analysis from SPOL. The change in fault parameters based on the attained sampling data set are stored in the vector.

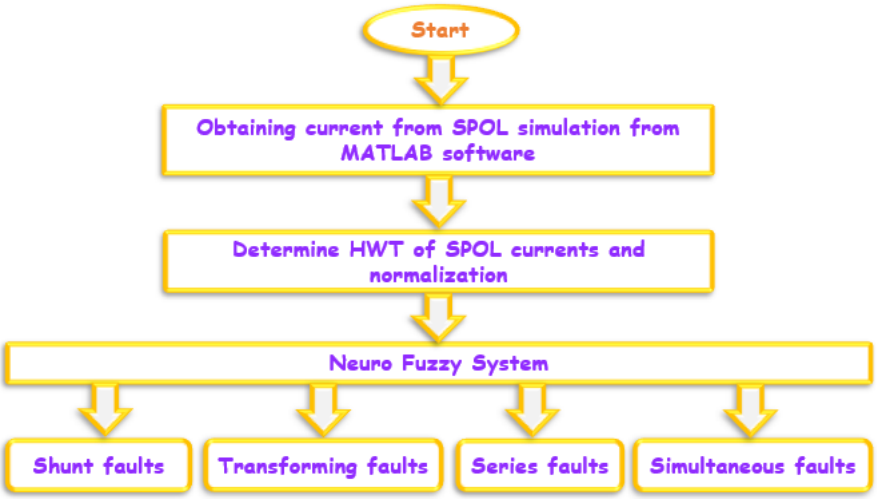

Fig. 7. Flow diagram of proposed work.

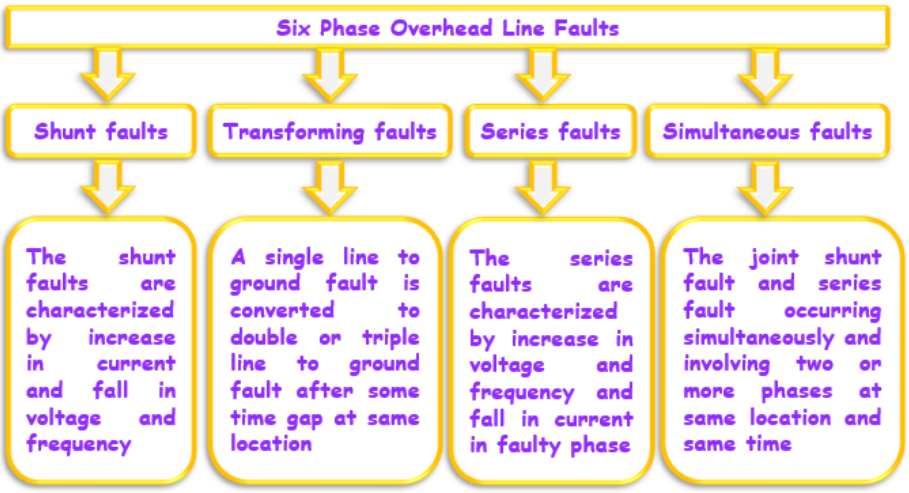

Fig. 8. Possible faults in SPOL.

3. NEURO FUZZY SYSTEM

Jang Roger was introduced to the NFS in 1993. Based on the input data and output data, NFS is a potent designing instrument for complex problems. To avoid the ANN and FL drawbacks, the globally applicable control design, i.e., NFS, was developed. NFS is accomplished by optimally combining ANN and FL. This combo allows both numerical and intelligent methods to be used. NFS has the potential to be applied in many other areas as well,

such as image recognition, weather forecasting, control systems and power systems. The Takagi Sugeno fuzzy inference system, which forms the basis for the NFS design can be classified into two types: antecedents and consequences. As illustrated in Fig. 9, the NFS architecture is divided into five layers. The proposed NFS consists of five layers compared to the traditional NFS. The architecture is briefly explained as follows.

Layer-1: Fuzzification layer- all inputs are multiplied by a transfer function to give the degree of organization.

Layer-2: Product layer (π)- all stages of membership are standardized.

Layer-3: Normalized layer (N)- normalized by the sum of weights of all neurons.

Layer-4: Defuzzification layer- the total weight of if-then rules is calculated.

Layer-5: Total output/summation layer- a single neuron which is the summation of all inputs.

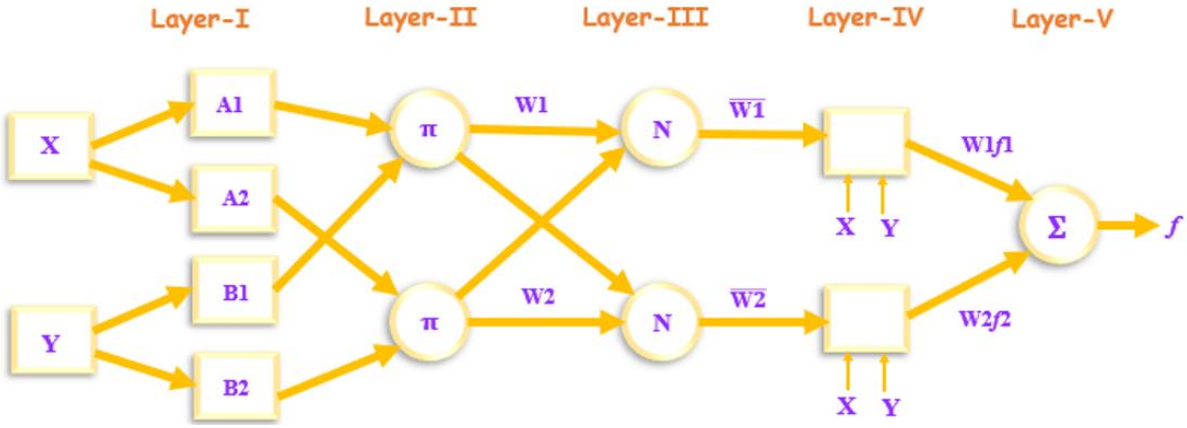

Fig. 9. Five-layer structure of NFS.

The NFS starts its operation by preparing the inputs (six phase HWT currents) and one output (fault location). In this work, 20 % of the data set was employed for training the NFS while 80 % was applied for testing its competency and accuracy. Initially, the HWT current are considered as inputs for training of NFS, and each input-output is fuzzified with membership functions. 3035×9 matrix was generated for NFS training data. The next step is the formation of the FL. The NFS is achieved from the structure of Takagi Sugeno system in MATLAB software. Consider a rule base that has 11 if-then rules. Then, the number of epochs and percentage of training data are described for training the NFS model. During the training phase parameters are updated according to the error information between the actual output values and the predicted values. After the training process, the input data set, the five-layer MATLAB Simulink construction of the NFS is obtained, and it is illustrated in Fig. 10. In the last step, compliance of the input parameter for the location result is obtained. Now NFS can allow the HWT currents and ready to locate shunt, transforming faults, series faults and simultaneous faults.

4. EXPERIMENTAL RESULTS

In this section, the performance of NFS has been tested on the SPOL with wide changes in all the fault parameters such as fault resistance (0 Ω - 80 Ω), location (1 km – 68 km) and inception angle (0° - 360°) for all shunt, transforming, series and simultaneous faults. The

validation process involves quantifying the effectiveness of the optimal HWT-NFS for location of faults. Based on the nature of fault type, NFS is monitored for fault locator in four patterns shunt, transforming, series and simultaneous faults. The performance of the NFS on the testing dataset summarised. The test results reflect the efficacy of the HWT-NFS in achieving better MFLE. Total 50000 test cases, the NFS is able to locate the occurrence of faults well within the maximum response time (MRT) threshold limit of half cycle (< 17 ms). The MFLE of fault location for all testing samples is expressed from the Eq. (1). The performance of NFS based scheme and comparative study is explained in the following subsections.

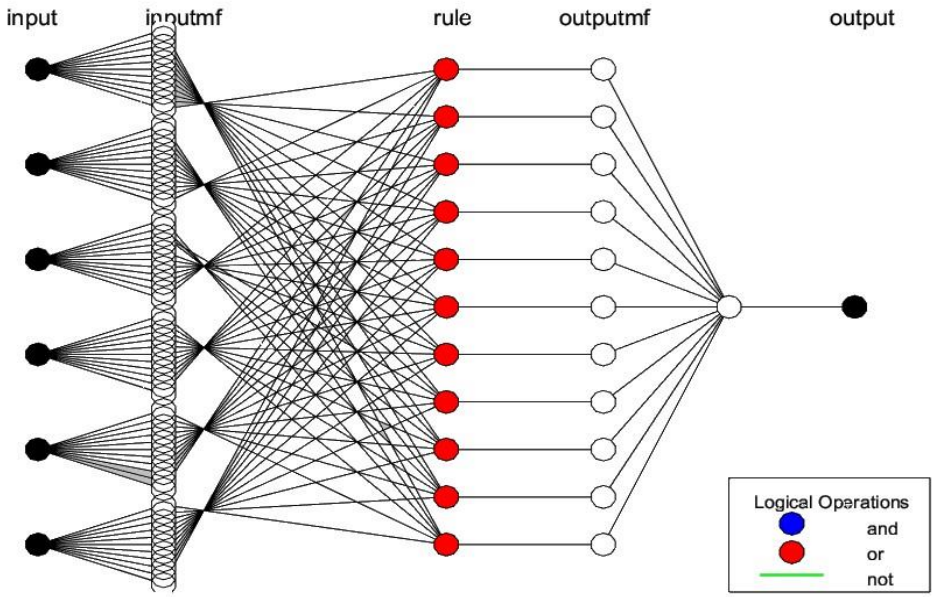

Fig. 10. NFS structure after training.

4.1. Performance of NFs Under Shunt Faults

Most of the faults in SPOL are shunt faults. Primary aim of fault location is shunt fault then transforming, series and simultaneous faults. The NFS locator has been verified on SPOL for around 10000 shunt faults. As can be seen from Table 1, the actual MFLE and estimated MFLE values for different inception angles, fault resistance and shunt faults. The final result illustrates that NFS is able to locate all shunt faults exactly and the MFLE is less than 0.261 %. Thus, one can understand that relay can locate the shunt faults in SPOL correctly and variation in fault parameters have a negative effect on the MFLE.

$$\text{MFLE } (\%) = \left| \frac{\text{Actual fault location} - \text{Estimated fault location}}{\text{SPOL length}} \right| \times 100 \quad (1)$$

4.2. Performance of NFS Under Transforming Faults

Location transforming faults is challenging due to the fault type changes shortly after the fault initiation. In this regard, there is a need for estimation on location of transforming faults. These are also checked with the NFS as well for 10000 samples. These faults are simulated on the SPOL for fault resistance, fault locations and fault inception angles. From Table 2. It can be concluded that the NFS has MFLE up to 0.248 % for all the transforming fault cases. On the other hand, the NFS identified this fault location perfectly. Hence it can be conformed that the NFS based technique is not affected by fault parameter variation.

Table 1. Test results of NFS under shunt faults for different fault parameters.

Parameter	Fault Type	Fault inception angle [°]	Fault resistance [Ω]	Actual fault location [km]	Estimated fault location [km]	MFLE [%]	MRT [ms]
Shunt faults are changing and actual fault location, fault inception angle, fault resistance is constant.	Fg	315	32	18	18.102	0.150	13.1
	EF	315	32	18	17.931	0.101	12.5
	DEFg	315	32	18	18.115	0.169	16.1
	ADE	315	32	18	18.005	0.007	15.7
	CDEFg	315	32	18	18.024	0.035	15.2
	BCDEF	315	32	18	17.971	0.042	13.2
	ABCDEFg	315	32	18	18.182	0.026	14.6
Actual fault location is changing and fault type, fault inception angle, fault resistance is fixed.	BEF	60	21	4	04.131	0.192	09.8
	BEF	60	21	12	12.012	0.017	11.4
	BEF	60	21	26	25.922	0.114	12.2
	BEF	60	21	38	37.888	0.164	13.6
	BEF	60	21	42	42.061	0.089	11.8
	BEF	60	21	52	52.015	0.022	11.6
	BEF	60	21	61	61.112	0.164	13.3
Fault inception angle is changing and fault type, actual fault location, fault resistance is fixed.	ABDEFg	45	10	63	63.123	0.180	15.4
	ABDEFg	135	10	63	63.178	0.261	12.5
	ABDEFg	225	10	63	63.145	0.213	12.1
	ABDEFg	270	10	63	63.098	0.144	14.7
	ABDEFg	315	10	63	63.043	0.063	08.9
	ABDEFg	330	10	63	63.142	0.208	06.0
	ABDEFg	360	10	63	63.168	0.247	11.5
Fault resistance is changing and actual fault location, fault type, fault inception angle is fixed.	CE	120	13	24	24.131	0.192	13.5
	CE	120	23	24	24.138	0.202	15.4
	CE	120	33	24	24.069	0.101	13.8
	CE	120	43	24	24.124	0.188	11.6
	CE	120	53	24	24.023	0.033	12.6
	CE	120	63	24	24.143	0.210	12.1
	CE	120	73	24	24.022	0.032	15.8

4.3. Performance Of NFS Under Series Faults

The series of faults have adverse effects on fault location in SPOL system MFLE because they are characterized by fall in current in the faulted lines. During fault location estimation, it is necessary to consider series faults disturbance. The NFS has been tested with 10000 series faults to verify its MFLE. For this purpose, the results have been replicated with various fault resistance, fault locations and fault inception angles and then they are tabulated in Table 3. It is confirmed that fault identification is still within 17 ms time, therefore no significant effect is observed, while for directional relaying also the MFLE remains well up to 0.251%.

Table 2. Test results of NFS under transforming faults for different fault parameters.

Parameters	Fault Type	Fault inception angle [°]	Fault resistance [Ω]	Actual fault location [km]	Estimated fault location [km]	MFLE [%]	MRT [ms]
Transforming faults are changing and actual fault location, fault inception angle, fault resistance is constant.	Cg to Fg	240	06	54	54.010	0.014	12.7
	BEg to Fg	240	06	54	54.096	0.135	15.1
	CDEg to Fg	240	06	54	54.123	0.180	11.3
	ADEg to Fg	240	06	54	53.966	0.064	07.6
	BCDEg to Fg	240	06	54	54.165	0.242	16.1
	ACDEg to Fg	240	06	54	53.876	0.182	15.6
	ABCDE to Fg	240	06	54	54.164	0.164	11.2
Actual fault location is changing and fault type, fault inception angle, fault resistance is fixed.	BCDg to Eg	110	44	6	6.005	0.007	13.8
	BCDg to Eg	110	44	18	18.133	0.195	12.1
	BCDg to Eg	110	44	24	23.944	0.082	15.5
	BCDg to Eg	110	44	33	32.988	0.017	10.3
	BCDg to Eg	110	44	43	43.130	0.191	15.1
	BCDg to Eg	110	44	54	55.912	0.129	10.3
	BCDg to Eg	110	44	61	61.113	0.166	11.2
Fault inception angle is changing and fault type, actual fault location, fault resistance is fixed.	Ag to Dg	25	78	27	27.169	0.248	13.9
	Ag to Dg	75	78	27	26.871	0.189	10.2
	Ag to Dg	125	78	27	27.121	0.177	14.4
	Ag to Dg	125	78	27	27.006	0.008	05.3
	Ag to Dg	175	78	27	27.117	0.172	11.8
	Ag to Dg	225	78	27	27.018	0.026	16.8
	Ag to Dg	275	78	27	26.924	0.111	13.3
Fault resistance is changing and actual fault location, fault type, fault inception angle is fixed.	CEg to Fg	80	5	11	10.882	0.173	14.1
	CEg to Fg	80	12	11	11.105	0.154	10.3
	CEg to Fg	80	15	11	10.901	0.145	11.9
	CEg to Fg	80	24	11	11.153	0.225	12.7
	CEg to Fg	80	36	11	11.097	0.142	11.0
	CEg to Fg	80	42	11	11.166	0.244	13.5
	CEg to Fg	80	51	11	11.150	0.220	14.1

4.4. Performance of NFS Under Simultaneous Faults

The simultaneous faults are failed to locate using the traditional techniques because series and shunt faults occur in SPOL different phases at the same location and same time. Thus, it is important to locate the simultaneous faults in SPOL. There has not been a satisfactory result to locating simultaneous faults on SPOL until now. The feasibility of NFS locator is checked for 10000 simultaneous fault simulated test cases. The MFLE calculations under simultaneous faults are listed in Table 4. According to the test simulations, it gives MFLE within 0.257%. It can be noted, corresponding simultaneous faults, the NFS locator is found to correctly locate the irrespective fault parameters.

Table 3. Test results of NFS under series faults for different fault parameters.

Parameters	Fault Type	Fault inception angle [°]	Fault resistance [Ω]	Actual fault location [km]	Estimated fault location [km]	MFLE [%]	MRT [ms]
Series faults are changing and actual fault location, fault inception angle, fault resistance is constant.	e	40	01	07	06.899	0.148	09.9
	de	40	01	07	07.168	0.247	12.4
	cef	40	01	07	07.177	0.260	12.3
	bdef	40	01	07	06.906	0.138	14.6
	acdef	40	01	07	06.870	0.191	11.8
	bcdef	40	01	07	07.101	0.148	11.3
	abcdef	40	01	07	07.030	0.044	14.3
Actual fault location is changing and fault type, fault inception angle, fault resistance is fixed.	def	130	14	08	08.166	0.244	15.5
	def	130	14	22	21.990	0.147	15.4
	def	130	14	22	22.169	0.248	12.1
	def	130	14	37	37.127	0.186	02.8
	def	130	14	43	42.829	0.251	11.6
	def	130	14	58	58.169	0.248	11.8
	def	130	14	64	64.061	0.089	16.8
Fault inception angle is changing and fault type, actual fault location, fault resistance is fixed.	bdef	35	36	45	44.842	0.232	10.4
	bdef	85	36	45	44.931	0.101	15.1
	bdef	135	36	45	45.189	0.266	12.8
	bdef	185	36	45	45.120	0.176	11.7
	bdef	235	36	45	45.055	0.080	12.7
	bdef	255	36	45	45.145	0.213	12.7
	bdef	285	36	45	45.096	0.141	14.8
Fault resistance is changing and actual fault location, fault type, fault inception angle is fixed.	ef	250	7	28	28.084	0.123	03.4
	ef	250	17	28	28.115	0.169	14.5
	ef	250	27	28	28.068	0.100	12.9
	ef	250	37	28	28.117	0.172	14.7
	ef	250	47	28	27.992	0.011	14.7
	ef	250	57	28	28.151	0.222	08.9
	ef	250	67	28	28.106	0.155	11.9

4.5. Performance of NFS with Far-End and Near-End Faults

The traditional location methods can identify up to 70–80% of the SPOL length. Therefore, it cannot identify the faults that occur between 80% and 100% of the SPOL length. Thus, it is important to examine the NFS application for near-end (1–3 km) and far-end (65–68 km) faults because the fault currents are different, which leads to NFS relay failures.

In view of this, the NFS is tested for a total of 10000 fault types near buses by changing the fault location in steps of 0.5 km. For all test simulations, the NFS performs the intended task of MFLE within 0.248. Some simulation results along with MFLE are listed in Table 5. It can be concluded that the NFS can locate far end and near-end faults rapidly.

Table 4. Test results of NFS under simultaneous faults for different fault parameters.

Parameters	Fault Type	Fault inception angle [°]	Fault resistance [Ω]	Actual fault location [km]	Estimated fault location [km]	MFLE [%]	MRT [ms]
Simultaneous faults are changing and actual fault location, fault inception angle, fault resistance is constant.	Ag and f	320	09	62	62.021	0.030	14.8
	Bg and e	320	09	62	61.891	0.160	12.0
	Cg and d	320	09	62	62.066	0.097	08.5
	Dg and c	320	09	62	62.877	0.180	14.2
	Fg and a	320	09	62	62.129	0.189	15.3
	Eg and b	320	09	62	62.103	0.151	16.1
	Fg and a	320	09	62	62.122	0.179	16.8
Actual fault location is changing and fault type, fault inception angle, fault resistance is fixed.	DF and e	70	23	09	09.144	0.211	11.1
	DF and e	70	23	19	18.161	0.236	12.2
	DF and e	70	23	29	29.108	0.158	11.2
	DF and e	70	23	39	39.152	0.223	10.6
	DF and e	70	23	49	48.947	0.077	16.1
	DF and e	70	23	59	59.115	0.169	12.9
	DF and e	70	23	61	61.102	0.150	10.4
Fault inception angle is changing and fault type, actual fault location, fault resistance is fixed.	CE and ad	15	35	47	46.911	0.130	10.2
	CE and ad	15	35	47	46.851	0.219	09.1
	CE and ad	65	35	47	47.092	0.135	01.8
	CE and ad	115	35	47	46.854	0.214	16.1
	CE and ad	165	35	47	47.160	0.235	14.7
	CE and ad	215	35	47	47.088	0.129	07.1
	CE and ad	265	35	47	47.106	0.155	16.3
Fault resistance is changing and actual fault location, fault type, fault inception angle is fixed.	Bg and d	100	06	17	17.175	0.257	10.1
	Bg and d	100	16	17	17.160	0.235	10.5
	Bg and d	100	26	17	17.023	0.033	16.9
	Bg and d	100	36	17	17.100	0.147	16.1
	Bg and d	100	46	17	17.111	0.163	11.5
	Bg and d	100	56	17	16.835	0.245	16.5
	Bg and d	100	66	17	17.168	0.247	13.7

4.6. Comparison Study

A summary results of the comparison performance assessment of the proposed NFS with other location schemes available in literature survey is explained in Table 6. Most of the methods reported in Table-6 have not illustrated regarding the transforming faults, series faults and simultaneous faults. The maximum difference between actual value and measured location value in [7, 26, 38, 39] are 0.533 km, 0.34 km, 0.69 km, and 0.25 km respectively. As revealed from the test results, the NFS raised better performance for shunt, transforming, series and simultaneous faults with the maximum difference between actual and measured location value level of 0.178, 0.169, 0.171 km and 0.175 km for shunt, transforming, series and simultaneous faults, respectively. In many cases, the NFS takes one cycle detection time to locate the fault compared to other schemes listed in Table 6. It can be observed that the MRT required by the proposed NFS to locate the faults is in half cycle (17 ms). Furthermore, the NFS is robust to far-

end and near-end faults, and moreover it can work well for other fault location also. In addition, the performance is unaffected by wide variations in resistance, location type and inception angle of fault which are not mentioned by earlier published algorithms. The MFLE of NFS shunt, transforming, series and simultaneous faults are 0.261%, 0.248 %, 0.251%, and 0.257 %, respectively. The result describes enhanced MLFE of the NFS compared to the existing technique.

Table 6. Comparison study with other schemes.

Parameter	Ref.				
	[7]	[28]	[40]	[41]	Proposed
Algorithm used	ANN	FL	FL	FL	NFS
Fault type	Shunt faults	Transforming faults	Shunt, series and simultaneous faults	Shunt, series and simultaneous faults	All faults
Line Type	SOTL	SOTL	Double circuit line	SOTL	SOTL
Inputs used	Wavelet Voltages and currents	DFT currents	Voltages and Currents	DFT currents	HWT currents
MFLE	0.688 %	0.5 %	1 %	0.4 %	0.261 %
MRT	one cycle time	-	-	-	17 ms

5. CONCLUSIONS

Accurate fault location in any transmission line is the key to the rapid restoration of fault line. Therefore, location of such faults in the SPOL should ensure the flawless power system operation. This study proposes an NFS based paradigm for fault location in SPOL. The process is initiated by sending the currents and preprocessing through HWT to obtain the normalized currents. These are employed to build the NFS for location of faults. Also, the change in fault locations, fault resistances, fault types and inception angles do not affect the location process. The HWT-NFS proposed scheme was demonstrated to be very robust, yielding a 100% accuracy rate. According to the simulation results, the NFS has a location MFLE of 0.261%. The effectiveness of the NFS was verified by MATLAB simulation setup. The sensitivity study demonstrated that the NFS is much more reliable, accurate, efficient, cost-effective and highly useful to be deployed in comparison to other techniques with an MFLE.

REFERENCES

[1] Q. Li, Y. Li, S. Rowland, J. Hu, I. Cotton, X. Jiang, "Audible noise evaluation for six-phase overhead lines transformed from existing three-phase double circuit infrastructures with uprated voltages," *High Voltage*, vol. 7, no. 5, pp. 866–876, 2022, doi: 10.1049/hve2.12246.

[2] N. Mishra, Z. Husain, A. Mukhraiya, "Novel six-phase DFIG suitable for three-phase and six-phase grid-connected disperse generation," IEEE Electric Power and Energy Conference, 2020, doi: 10.1109/EPEC48502.2020.9320093.

[3] T. Yacob, Z. Zakaria, N. Hamzah, "Study of six phase transmission line using the autotransformer conversion," IEEE Student Conference on Research and Development, 2011, doi: 10.1109/SCOReD.2011.6148736.

[4] J. Stamp, A. Girgis, "Fault location technique for six phase transmission lines with unsynchronized phasors," IEEE Conference on Transmission and Distribution, 1999, doi: 10.1109/TDC.1999.756130.

[5] J. Stamp, A. Girgis, "Fault location and phase selection for UHV six-phase transmission lines," IEEE Asia Pacific Power and Energy Engineering Conference, 2011, doi: 10.1109/APPEEC.2011.5748603.

[6] T. Althi, E. Koley, S. Ghosh, D. Mohanta, "A random forest based communication-less approach for protection scheme of six-phase transmission line against shunt, series, evolving and cross-country faults," *Electrical Engineering*, vol. 105, pp. 4157–4175, 2023, doi: 10.1007/s00202-023-01929-w.

[7] E. Koley, K. Verma, S. Ghosh, "An improved fault detection classification and location scheme based on wavelet transform and artificial neural network for six phase transmission line using single end data only," *SpringerPlus*, vol. 4, p. 551, 2015, doi: 10.1186/s40064-015-1342-7.

[8] S. Warathe, R. Patel, "Six-phase transmission line over current protection by numerical relay," International Conference on Advanced Computing and Communication Systems, 2015, doi: 10.1109/ICACCS.2015.7324102.

[9] G. Kapoor, "A mathematical morphology-based fault detection and faulty phase categorization scheme for the protection of six-phase transmission line," *Jordan Journal of Electrical Engineering*, vol. 6, no. 1, pp. 35-48, 2020, doi: 10.5455/jjee.204-1581015401.

[10] G. Kapoor, A. Yadav, "A single-terminal hybrid scheme for six-phase transmission line protection," IEEE International Conference on Power Electronics, Drives and Energy Systems, 2020, doi: 10.1109/PEDES49360.2020.9379377.

[11] G. Kapoor, "Six phase transmission line boundary protection using wavelet transform," IEEE India International Conference on Power Electronics, 2018, doi: 10.1109/IICPE.2018.8709439.

[12] B. Pierre, "High phase order transmission line fault types," *Electric Power Components and Systems,* vol. 47, no. 18, pp. 1667–1676, 2019, doi: 10.1080/15325008.2019.1689456.

[13] A. Kumar, M. Kumar, M. Ramesha, B. Gururaj, A. Srikanth, "Support vector machine based fault section identification and fault classification scheme in six phase transmission line," *IAES International Journal of Artificial Intelligence,* vol. 10, no. 4, pp. 1019-1024, 2021, doi: 10.11591/ijai.v10.i4.pp1019-1024.

[14] T. Althi, E. Koley, S. Ghosh, S. Shukla, "Six phase transmission line protection using Bat algorithm tuned stacked sparse autoencoder," *Electric Power Components and Systems*, vol. 51, no. 2, pp. 113-130, doi: 10.1080/15325008.2022.2163519.

[15] A. Rao, E. Koley, S. Ghosh. "An optimally tuned rotation forest-based local protection scheme for detecting high-impedance faults in six-phase transmission line during nonlinear loading," *Iranian Journal of Science and Technology, Transactions of Electrical Engineering*, vol. 46, pp. 1129-1147, 2022, doi: 10.1007/s40998-022-00515-3.

[16] T. Althi, E. Koley, S. Ghosh, "Protection of six-phase transmission line using recursive estimation of non-linear autoregression model coefficients and decision tree," *IET Science, Measurement & Technology*," vol. 14, no. 10, pp. 931-942, 2021, doi: 10.1049/iet-smt.2019.0282.

[17] C. Asbery, Y. Liao, "Fault identification on electrical transmission lines using artificial neural networks," *Electric Power Components and Systems,* vol. 49, no. 13-14, pp. 1118-1129, 2021, doi: 10.1080/15325008.2022.2049659.

[18] A. Swetapadma, A. Yadav, "A novel single-ended fault location scheme for parallel transmission lines using k-nearest neighbor algorithm," *Computers & Electrical Engineering,* vol. 69, pp. 41-53, 2018, doi: 10.1016/j.compeleceng.2018.05.024.

[19] M. Tuka, "Investigation of voltage dip problems during faults on a grid-tied doubly fed induction generator in a wind energy system," *Jordan Journal of Electrical Engineering*, vol. 9, no. 2, pp. 209-227, 2023, doi: 10.5455/jjee.204-1669028936.

[20] Z. Mrabet, N. Sugunaraj, P. Ranganathan, S. Abhyankar, " Random forest regressor-based approach for detecting fault location and duration in power systems," *Sensors,* vol. 22, no. 2, p. 458, 2022, doi: 10.3390/s22020458.

[21] I. Murugesan, P. Gunasekaran, S. Muthusamy, P. Ramamoorthi, "A normalized Haar wavelet transformation based firefly optimization algorithm for power transmission line fault detection problems," *Energy Sources, Part A: Recovery, Utilization, and Environmental Effects,* vol. 45, no. 2, pp. 4965-4981, 2023, doi: 10.1080/15567036.2023.2206797.

[22] S. Ekici, "Support vector machines for classification and locating faults on transmission lines," *Applied Soft Computing*, vol. 12, no. 6, pp. 1650-1658, 2012, doi: 10.1016/j.asoc.2012.02.011.

[23] G. Raju, N. Srikanth, "Mono ANN module protection scheme and multi ann modules for fault location estimation for a six-phase transmission line using discrete wavelet transform," *Journal of Operation and Automation in Power Engineering,* vol. 12, no. 4, pp. 337-351 2023, doi: 10.22098/JOAPE.2023.11690.1874.

[24] J. Xiangqing, L. Yuan. "Accurate location of evolving faults on transmission lines using sparse wide area measurements" *International Journal of Emerging Electric Power Systems,* vol. 19, no. 1, p. 20170244, 2018, doi: 10.1515/ijeeps-2017-0244.

[25] V. Ashok, A. Yadav, V. Naik, "Fault detection and classification of multi-location and evolving faults in double-circuit transmission line using ANN," Advances in Intelligent Systems and Computing, 2021, doi: 10.1007/978-981-13-0514-6_31.

[26] S. Kulkarni, S. Santoso, "Time-domain algorithm for locating evolving faults," *IEEE Transactions on Smart Grid*, vol. 3, no. 4, pp. 1584-1593, 2012, doi: 10.1109/TSG.2012.2207469.

[27] X. Jiao, Y. Liao, "An analytical approach to locate evolving faults on transmission lines based on sparse wide area measurements," IEEE Power and Energy Conference, 2017, doi: 10.1109/PECI.2017.7935721.

[28] A. Kumar, M. Chakravarth, "Fuzzy inference system based distance estimation approach for multi location and transforming phase to ground faults in six phase transmission line," *International Journal of Computational Intelligence Systems,* vol. 11, no. 1, pp. 757–769, 2018, doi: 10.2991/ijcis.11.1.58.

[29] A. Swetapadma, A. Yadav, "All shunt fault location including cross-country and evolving faults in transmission lines without fault type classification," *Electric Power Systems Research,* vol. 123, pp. 1-12, 2015, doi: 10.1016/j.epsr.2015.01.014.

[30] S. Shukla, E. Koley, S. Ghosh, "Detection and classification of open conductor faults in six-phase transmission line using wavelet transform and naive bayes classifier," IEEE International Conference on Computational Intelligence and Computing Research, 2017, doi: 10.1109/ICCIC.2017.8524343.

[31] M. Abasi, N. Heydarzadeh, A. Rohani, "Broken conductor fault location in power transmission lines using gmdh function and single-terminal data independent of line parameters", *Journal of Applied Research in Electrical Engineering,* vol. 1, no. 1, pp. 22–32, 2021, doi: 10.22055/jaree.2021.35473.1012.

[32] A. Swetapadma, A. Yadav, "Fuzzy based fault location estimation during unearthed open conductor faults in double circuit transmission line," Information Systems Design and Intelligent Applications, 2016, doi: 10.1007/978-81-322-2752-6_44.

[33] B. Rashad, D. Ibrahim, M. Gilany, A. Gharably, "Adaptive single-end transient-based scheme for detection and location of open conductor faults in HV transmission lines," *Electric Power Systems Research*, vol. 182, p. 106252, 2020, doi: 10.1016/j.epsr.2020.106252.

[34] P. Xu, G. Wang, H. Li, Y. Liang, P. Zhang, "A new method for open conductors fault calculation of four-parallel transmission lines," Asia-Pacific Power and Energy Engineering Conference, 2010, doi: 10.1109/APPEEC.2010.5449306.

[35] A. Baghdadi, M. Abd, F. Flaih, "A new detection method for load side broken conductor fault based on negative to positive current sequence," *Electronics*, vol. *11*, no. 6, p. 836, 2022, doi: 10.3390/electronics11060836.

[36] J. Che, T. Kim, S. Pyo, J. Park, B. An, T. Park, "Prevention of wildfires using an ai-based open conductor fault detection method on overhead line," *Energies*, vol. 16, no. 5, p. 2366, 2023, doi: 10.3390/en16052366.

[37] D. Tailor, V. Makwana, "Analysis of simultaneous broken and fallen to earth conductor fault condition in power systems, " *IETE Journal of Education*, vol. 64, no. 1, 34-40, 2023, doi: 10.1080/09747338.2022.2090454.

[38] D. Tailor, V. Makwana, "Analysis of faulted power system during simultaneous open conductor and ground fault," *IET Generation, Transmission & Distribution*, vol. 14, no. 22, pp. 5319-5326, 2020, doi: 10.1049/iet-gtd.2019.1211.

[39] B. Bhut, R. Sharma, "Analysis of simultaneous ground and phase faults on a six phase power system, " *IEEE Transactions on Power Delivery*, vol. 4, no. 3, pp. 1610-1616, 1989, doi: 10.1109/61.32650.

[40] A. Swetapadma, A. Yadav, "Fuzzy inference system approach for locating series, shunt, and simultaneous series-shunt faults in double circuit transmission lines," *Computational Intelligence and Neuroscience*, 2015, doi: 10.1155/2015/620360.

[41] A. Kumar, C. Sanjay, M. Chakravarth, "Six phase transmission line protection against open conductor, phase to ground and simultaneous faults using fuzzy inference system Transmission Line," *International Journal of Computational Intelligence Studies,* vol. 8, no. 3, pp. 245 - 267, 2019, doi:10.1504/IJCISTUDIES.2019.102626.

[42] H. Abd El-Ghany, A. Azmy, A. Abeid, "A general travelling-wave-based scheme for locating simultaneous faults in transmission lines," *IEEE Transactions on Power Delivery,* vol. 35, no. 1, pp. 130-139, 2020, doi: 10.1109/TPWRD.2019.2931178.

[43] V. Makwana, B. Bhalja, "A new digital distance relaying scheme for series-compensated double-circuit line during open conductor and ground fault," *IEEE Transactions on Power Delivery*, vol. 27, no. 2, pp. 910-917, 2012, doi: 10.1109/TPWRD.2011.2178438.

[44] A. Kumar, N. Sitharamaiah, M. Chakravarthy, " Series capacitor-compensated double-circuit transmission line directional relay system using a fuzzy expert system with a Haar wavelet," *Iran Journal of Computer Science*, vol. 5, no. 18, pp. 157–166, 2022, doi: 10.1007/s42044-021-00097-z.

[45] J. Reddy, D. Mohanta, "Adaptive-neuro-fuzzy inference system approach for transmission line fault classification and location incorporating effects of power swings," *IET Generation, Transmission & Distribution,* vol. 2, no. 2, pp. 235–244, 2008, doi: 10.1049/iet-gtd:20070079.

[46] T. Mohsen, S. Javad, "Fault location in series-compensated transmission lines using adaptive network-based fuzzy inference system," *Electric Power Systems Research*, vol. 208, p. 107800, 2022, doi: 10.1016/j.epsr.2022.107800.

[47] M. Mustaria , M. Hashima , M. Osmana, A. Ahmada, F. Ahmada , M. Ibrahima, "Fault location estimation on transmission lines using neuro-fuzzy system," *Procedia Computer Science,* vol. 163, pp. 591–602, 2019, doi: 10.1016/j.procs.2019.12.141.

[48] T. Kawady, G. Sowilam, R. Shalwala, "Improved distance relaying for double-circuit lines using adaptive neuro-fuzzy inference system," *Arabian Journal for Science and Engineering*, vol. 45, pp. 1969–1984, 2020, doi: 10.1007/s13369-020-04369-x.

[49] E. Eldin, "Fault location for a series compensated transmission line based on wavelet transform and an adaptive neuro-fuzzy inference system," Electric Power Quality and Supply Reliability Conference, 2010, doi: 10.1109/PQ.2010.5549994.

[50] J. Sadeh, H. Afradi, "A new and accurate fault location algorithm for combined transmission lines using Adaptive Network-Based Fuzzy Inference System," *Electric Power Systems Research*, vol. 79, no. 11, pp. 1538-1545, 2009, doi: 10.1016/j.epsr.2009.05.007.

[51] H. Eristi, "Fault diagnosis system for series compensated transmission line based on wavelet transform and adaptive neuro-fuzzy inference system," *Measurement*, vol. 46, no. 1, pp. 393-401, 2013, doi: 10.1016/j.measurement.2012.07.014.

[52] C. Jung, K. Kim, J. Lee, B. Klöckl, "Wavelet and neuro-fuzzy based fault location for combined transmission systems," *International Journal of Electrical Power & Energy Systems*, vol. 29, no. 6, pp.445–454, 2007, doi: 10.1016/j.ijepes.2006.11.003.

[53] A. Khaleghi, M. Sadegh, "Single-phase fault location in four-circuit transmission lines based on wavelet analysis using ANFIS," *Journal of Electrical Engineering & Technology,* vol. 14, pp.1577–1584, 2019, doi: 10.1007/s42835-019-00209-7.

[54] M. Paul, S. Debnath, "ANFIS based single line to ground fault location estimation for transmission lines," Michael Faraday IET International Summit, 2020, doi: 10.1049/icp.2021.1077.

[55] A. Kumar, P. Sridhar, T. Kumar, T. Babu, V. Mohan, "Adaptive neuro-fuzzy inference system based evolving fault locator for double circuit transmission lines," *IAES International Journal of Artificial Intelligence,* vol. 9, no. 3, pp. 448-455, 2020, doi: 10.11591/ijai.v9.i3.pp448-455.

[56] A. Kumar, C. Sanjay, M. Chakravarthy, "Adaptive neuro fuzzy inference system-based fault location technique in double circuit transmission line against simultaneous faults, "*Multiscale and Multidisciplinary Modeling, Experiments and Design,* vol. 3, pp.143–150, 2020, doi: 10.1007/s41939-019-00066-x.